

## Fractal Growth from Local Instabilities

RAFFAELE CAFIERO<sup>1</sup> AND GUIDO CALDARELLI<sup>2</sup>

<sup>1</sup> *PMMH Ecole Sup. de Physique et de Chimie Industrielles (ESPCI), 10, rue Vauquelin-75231 Paris Cedex 05 France*

<sup>2</sup> *Sezione INFM di Roma1 and Dipartimento di Fisica, Università "La Sapienza", P.le A.Moro 2 00185 Roma, Italy.*

(received ; accepted )

PACS. 61.43.Hv – Fractals; macroscopic aggregates (including diffusion-limited aggregates).

PACS. 68.35.Ja – Surface and interface dynamics and vibrations.

PACS. 81.10.Bk – Growth from vapor.

PACS. 64.60.Ht – Dynamic critical phenomena.

**Abstract.** – We study, both with numerical simulations and theoretical methods, a cellular automata model for continuum equations describing growth processes in the presence of an external flux of particles. As a result of local instabilities we find a fractal regime of growth for small external fluxes. The growing tip is selected with probability proportional to the curvature in the point. A parameter  $p$  gives the probability of lateral growth on the tip. The value of  $p$  determines the fractal dimension of the aggregate. Furthermore, for each value of  $p$  a cross-over between two different fractal dimensions is observed. Instead, the roughness exponent  $\chi$  of the aggregates does not depend on  $p$  ( $\chi \simeq 0.5$ ). Fixed scale transformation approach is applied to compute theoretically the fractal dimension for one of the branches of the structure.

From a technological point of view the growth by vapor atom deposition is the most common way to produce films [1]. It is known that local instabilities play a decisive role in the formation of patterns observed in experiments, such as grooves, mounds and metallurgical junctions [2]. These kinds of phenomena are usually described by the following continuum equation [3]

$$\dot{h}(x) = J - \xi \nabla^2 h(x), \quad (1)$$

where  $h(x)$  represents the surface height corresponding to the substrate coordinate  $x$ ;  $J$  is the incident flux of particles. The Laplacian term with the negative sign plays the role of an antidiusion, and it is responsible for the instability. The precise meaning of  $\xi$  depends on the particular kind of instability involved in the process. The  $J$  term in eq.(1) can be ruled out with a change of coordinates in a frame comoving with the surface. Then  $h$  can be considered just as the fluctuation around the average. The resulting equation is

$$\dot{h}(\vec{x}, t) = -\nabla^2 h(\vec{x}, t). \quad (2)$$

The solution of (2) in Fourier space is

$$h(\vec{k}, t) = h(\vec{k}, 0)e^{\xi \vec{k}^2 t}. \quad (3)$$

Therefore all the modes present at the origin are exponentially amplified. In order to control this instability, people usually introduce a term proportional to  $\nabla^4 h(x)$  in the eq. (1). This brings to

$$\dot{h}(\vec{k}, t) = \xi \vec{k}^2 h(\vec{k}, t) - \lambda \vec{k}^4 h(\vec{k}, t) \quad (4)$$

whose solution now is

$$h(\vec{k}, t) = h(\vec{k}, 0)e^{\xi \vec{k}^2 - \lambda \vec{k}^4 t}. \quad (5)$$

Therefore only the long wavelength modes are still unstable. The result of this process is the formation of columns separated by very deep grooves.

An alternative continuum approach is represented by the Reparametrization Invariant Formulation of the surface growth equation [4]. The basic idea is that the growth of surfaces only depends on its intrinsic properties. Therefore eq.(1) can be rewritten as

$$\dot{\vec{r}} = \hat{n}(J - \xi H) \quad (6)$$

where  $\vec{r}$  is the position vector of the surface,  $\hat{n}$  the local normal unit vector and  $H$  the local curvature.  $J$  and  $\xi$  are defined as before. Within this scheme the  $\nabla^4 h$  term is substituted by the Beltrami-Laplace operator for the curvature.

When the tips of two columns join together the deep groove below them disappears and the effective resulting surface is almost flat[5]. In this spirit, a simpler way to approach the study of surface growth is represented by the introduction of lattice models able to keep the relevant properties of the phenomenon. Many models have been proposed in the past years: the Eden model [6], ballistic deposition models[7], Solid-On-Solid (SOS) models [8] and others (for a review on surface growth models see also Ref.[9, 10]).

Here, we present a lattice model to verify the role of the surface curvature in these growth processes. Consider a surface subject to an incoming flux of particles. The model is based on the following two rules. Firstly, the probability that a particle stops in a given site is proportional to the local negative curvature of the surface. For each point the curvature is computed in a first approximation as the Laplacian function in the point. In this way, the growth probability at  $t$  on the tip  $\vec{x}, t$  is given by

$$P(x, t) \propto [2h(x, t) - h(x - 1, t) - h(x + 1, t)] \quad (7)$$

Secondly, a particle sticks right on the tip with probability  $p$  while with probability  $1 - p$  it can stick laterally. We introduce in this way the possibility to develop overhangs. Under this respect this model can be considered a generalization of the growth model proposed in Ref.[11] for sticky particles. The surface height  $h(i)$  on a site  $i$  corresponds to the position of the highest particle on that column. We will consider here the limit of vanishing external flux, which is mimicked allowing just one particle to stick at a time.

This model of aggregation does not give rise to compact structures, but instead to fractal ones merging themselves to form a continuous surface. In the system, every now and then, a tip whose value of the Laplacian operator becomes larger and larger, spans uniformly the system size. When the growth reaches a boundary there is a new flat surface where the deposition proceeds.

To reduce finite size effects, in our simulations we considered periodic boundary conditions along the horizontal direction of the system. In Fig.1 we present some typical patterns for

size  $L \times 2L$  ( $L = 256$ ) and for different values of  $p$ . There is a transient regime, that we call the *scaling regime* in analogy with the dielectric breakdown model (DBM) [12]. Here several branches compete with each other in the growth process. After that, in the *steady state*, a single branch prevails and grows forever. Due to the screening induced by the shadowing between competing branches, the system develops fractal properties in the scaling regime where we focus our studies. We have performed several numerical simulations of this model for different values of  $p$  and for system sizes up to  $L = 512$ , and height  $2L$ . The results presented here refer to average on about 100 realization for every value of  $p$  and  $L = 256, 512$ .

In this model the sample grows as a compact set of different columns as observed experimentally in [13, 14]. Authors, in [14], conjecture an exponential distribution for the tip height from their experimental results on columnar structured gold electrodeposits.

$$D(h) \propto \exp(-bh) \quad (8)$$

where  $b$  is the inverse of a characteristic length. The same shape of  $D(h)$  was previously observed in [13], through scanning tunneling microscopy analysis of vapor deposited gold films. We computed  $D(h)$  for our model with  $p = 1$ ,  $L = 256$  and maximum tip height  $h_{max} = 256, 512$ . The results reproduce the same exponential behavior of  $D(h)$  observed in [13, 14]. The characteristic height  $b^{-1}$  turns out to be actually proportional to the maximum height  $h_{max}$  ( $b^{-1} = c^{-1}h_{max} \sim \frac{h_{max}}{5}$ ).

In order to describe the clusters obtained we also focused on the roughness exponent  $\chi(p)$  of the surface. The roughness exponent is defined as the ensemble averaged width of the interface

$$W(l, t) = \langle (h(i, t) - \langle h(i, t) \rangle)^2 \rangle^{1/2} \sim l^\chi f(t^{1/z}/l) \quad (9)$$

where  $z$  is the dynamical exponent, the angular brackets denote the average over all portions of the interface of length  $l$  for a given realization of total length  $L$ , and over different realizations, and  $f$  is a scaling function such that  $f(y) \sim y^\chi$  for  $y \ll 1$  and  $f(y) = const$  for  $y \gg 1$ . The exponent  $\beta = \chi/z$  describes the transient roughening. In the asymptotic time limit on gets:

$$W(l, t = \infty) = W(l) \propto l^\chi \quad (10)$$

Interestingly enough, the value of this quantity does not depend on the value of  $p$  as one can see from Table I. A plot of this scaling is shown in Fig.2.

A dependence on  $p$  affects, instead, the fractal dimension of the aggregate. In our simulations we studied the lower strip where the growth process can be considered fully screened by the shadowing effect. In Fig.3 we show the plot of  $N(l)$ , number of occupied boxes of size  $l$ , versus  $l$  in the scaling regime for different values of  $p$ . In Tab.I we report the measured values for these exponents. The result is that the value of  $D_f$  strongly depends on the parameter  $p$ . Moreover, for all values of  $p$  a cross-over between two different fractal dimensions is observed. In particular the region of small  $l$  are characterized by a value of  $D_f^{low}$  changing from 1.20(3) to 1.08(3) as  $p$  passes from 0.1 to 0.9. Larger regions are characterized by a similar trend with the value of  $D_f^{high}$  changing from 1.30(3) to 1.12(3) as  $p$  passes from 0.1 to 0.9

As regards the trend of this variation one can conclude that in the limit  $p \rightarrow 1$  the growth is dominated by the highest tip that grows forever. In this condition the growth of the aggregate leaves large empty regions that strongly reduce the fractal dimension of the aggregate. The possibility of lateral growth instead, delays this effect in such a way to form an intermediate region where one can study non trivial fractal properties.

In order to obtain an analytical computation to reproduce the behavior of  $D_f^{low}$ , we used a theoretical scheme of a novel type that can deal with irreversible dynamic processes in a reasonably systematic way. The Fixed Scale Transformation (FST) [15] focuses on the dynamics at a given scale and allows to compute the nearest neighbors correlations at this

scale by lattice diagrams. The structure that we want to study becomes well defined in the following limits:

asymptotic time limit ( $t \rightarrow \infty$ ): only regions of the system where the growth is frozen are considered;

large scale limit ( $r \rightarrow \infty$ ) to avoid the presence of finite size effects

In the FST scheme, these two limits are reached through the fixed point convergence of the lattice diagrams after a certain order and considering the system at a coarse grained scale [16]. In order to perform the first limit one defines an elementary cell of two sites. The two configurations in Fig.4 are the only ones subject to growth, with an associated probability to have a transition from one to the other in the growth direction. The fixed point of the process (that can be regarded as the limit  $t \rightarrow \infty$ ) is obtained looking at the eigenvector corresponding to the eigenvalue 1 (which is also the largest one)

$$M \begin{pmatrix} C_1 \\ C_2 \end{pmatrix}^t = \begin{pmatrix} C_1 \\ C_2 \end{pmatrix}^{t+1} \quad (11)$$

where  $C_1$  and  $C_2$  are the probabilities of occurrence of configurations of the type 1 and 2 respectively.

The average number of boxes occupied by the structure in a change of scale  $l \rightarrow \frac{l}{2}$  is

$$\langle n \rangle = C_1 + 2C_2. \quad (12)$$

Since we are studying the intersection set between the structure and a line defining the growth front, the fractal dimension of the structure is simply

$$D_f = 1 + D_t \quad (13)$$

where  $D_t$  is the transverse fractal dimension related to  $\langle n \rangle$  by the formula:

$$D_t = \frac{\ln \langle n \rangle}{\ln(2)} = \frac{\ln(C_1 + 2C_2)}{\ln(2)}. \quad (14)$$

Given this theoretical framework, it is very easy to develop the calculations for the present case. Consider the graph in Fig.4; as a first approximation of the boundary conditions, one can consider the open ones, where the pattern has no other occupied sites around. The opposite condition is represented by the closed ones in which the entire pattern is replied. In both cases the growth probabilities are normalized to one inside the growth column. Usually, a satisfactory approximation consists in considering only these two limiting cases, where the two fixed value of the configuration probabilities are given by:

$$\begin{aligned} C_1^* &= \frac{M_{12}^{cl} + 2M_{21}^{cl} - \frac{3}{2}M_{21}^{op} - \sqrt{(\frac{3}{2}M_{21}^{op} - M_{12}^{cl} - 2M_{21}^{cl})^2 - 4AM_{21}^{cl}}}{2A} \\ C_2^* &= 1 - C_1^* \end{aligned} \quad (15)$$

where  $A = M_{12}^{cl} + M_{21}^{cl} - 3/2(M_{12}^{op} + M_{21}^{op})$ . By using the scheme shown in Fig.4 one obtains the values of the matrix elements in the FST scheme for open and closed boundary conditions.

$$M_{12}^{op} = \frac{1-p}{1+p} \quad ; \quad M_{11}^{op} = 1 - M_{12}^{op} \quad (16)$$

$$M_{21}^{op} = \frac{2p}{1+p} \quad ; \quad M_{22}^{op} = 1 - M_{21}^{op} \quad (17)$$

$$M_{12}^{cl} = 1 - p \quad ; \quad M_{11}^{cl} = 1 - M_{12}^{cl} \quad (18)$$

$$M_{21}^{cl} = p \quad ; \quad M_{22}^{cl} = 1 - M_{21}^{cl} \quad (19)$$

Two sources of screening are present in our model: one is due to the fact that only the tips can grow, and this is a local effect which is accounted for in the FST computation. The other, more important, is shadowing, which is highly non-local, depending on the whole structure of the aggregate. This effect cannot be easily accounted in the FST scheme [15]. This reflects on the results of the computation, especially for low values of  $p$ , where shadowing is more important. Instead for as  $p \rightarrow 1$  there is a reasonable agreement between the FST computation and numerical simulations (last column of Table I).

To conclude, we have presented a simple cellular automata model, which describes fractal surface growth in the limit of vanishingly small external flux, under the effect of a local instability. The model shows non-trivial, interesting fractal and roughness properties, which are studied both numerically and analytically. We acknowledge useful discussion with R. Ball, P. De Los Rios, A. Maritan, L. Pietronero, and the support of the European Network contract FMRXCT980183.

## REFERENCES

- [1] R. Messier and J. E. Yehoda, *J. Appl. Phys.* **58**, 3739 (1985); G. S. Bales, R. Bruinsma, E.A. Eklund, R. P.U. Karunasiri, J. Rudnick, A Zangwill, *Science* **249**, 264 (1990); C. W. Tu and J. S. Harris Jr., *J. Cryst. Growth* **111**, R9 (1991).
- [2] A.J. Arvia and R. C. Salvarezza,
- [3] R. Schwoebel and E. Shipsey, *J. Appl. Phys.* **37**, 3682 (1966); R. Schwoebel, *J. Appl. Phys.* **40**, 614 (1969).
- [4] M. Marsili, A. Maritan F. Toigo and J.R. Banavar, *Rev. Mod. Phys.* **68**, No. 4, 963 (1996).
- [5] P.De Los Rios, private communication.
- [6] N. M. Eden, *Proceedings of the Fourth Berkeley Symposium on Mathematics, Statistics and Probability*, F. Neymann ed., Vol. IV (UC-Berkeley, 1961).
- [7] M.J. Vold, *J. Phys. Chem.* **63**, 1608 (1959); M. J. Vold, *J. Phys. Chem* **64**, 1616 (1960).
- [8] J.M. Kim and J. M. Kosterlitz, *Phys. Rev. Lett.* **62**, 2289 (1989).
- [9] T. Halpin-Healey and Y-C. Zhang, *Phys. Rep.* **254**, 215 (1995).
- [10] A.-L. Barabasi and H. E. Stanley, *Fractal Concepts in Surface Growth*, Cambridge University Press, Cambridge, UK (1995).
- [11] P. Meakin and R. Julien, *PhysicaA* **175**, 211 (1991).
- [12] L. Niemeyer, L. Pietronero and H. J. Wiessmann, *Phys. Rev. Lett.* **52**, 1033 (1984).
- [13] P. Herrasti, P. Ocón, L. Vásquez, R. C. Salvarezza, J. M. Vara and A. J. Arvia, *Phys. rev. A* **45**, 7440 (1992).
- [14] M. E. Vela, S. L. Marchiano, R. C. Salvarezza, A. J. Arvia, *Journ. Electroan. Chem.* **388**, 133 (1995).
- [15] A. Erzan, L. Pietronero and A. Vespignani *Rev. Mod. Phys.* **67** n.3 (1995).
- [16] R. Cafiero, L. Pietronero and A. Vespignani, *Phys. Rev. Lett.* **70**, 3939 (1993)

TABLE I. – *Fractal dimension for the lower and upper scaling region and roughness exponent for different values of  $p$  and system size  $L = 256, 512$ .*

$p$	$D_f^{low}(p)$	$D_f^{high}(p)$	$\chi(p)$	$D_f^{low} FST(p)$
0.1	$1.20 \pm 0.03$	$1.30 \pm 0.03$	$0.54 \pm 0.03$	1.91
0.33	$1.18 \pm 0.03$	$1.28 \pm 0.03$	$0.55 \pm 0.04$	1.66
0.5	$1.17 \pm 0.03$	$1.24 \pm 0.02$	$0.50 \pm 0.02$	1.46
0.7	$1.14 \pm 0.02$	$1.20 \pm 0.02$	$0.48 \pm 0.04$	1.24
0.9	$1.08 \pm 0.02$	$1.12 \pm 0.02$	—	1.08

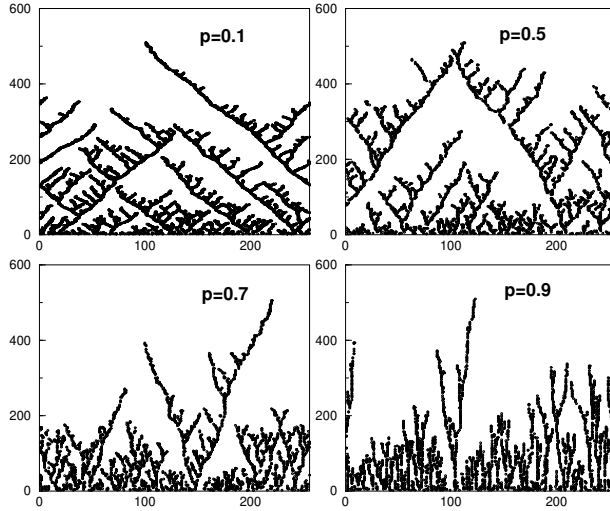


Fig. 1. – (a)-(d): Typical patterns for different values of  $p$  (the system size and the values of  $p$  are shown in the legends).

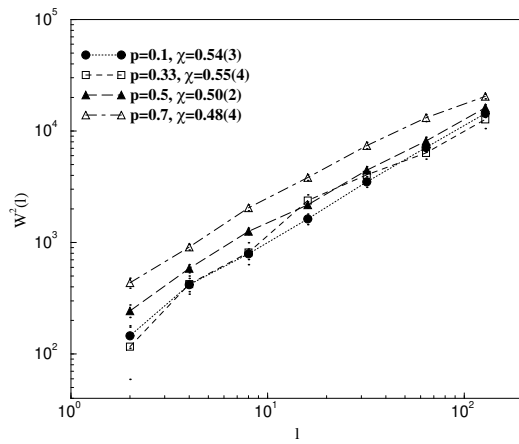


Fig. 2. – Scaling behavior of the squared width  $W^2(l)$  width of portions of size  $l$  of the aggregates surface, defined as the path of the highest occupied sites for each column, for different  $p$ . We get a roughness exponent  $\chi$  around  $1/2$  for all values of  $p$ .

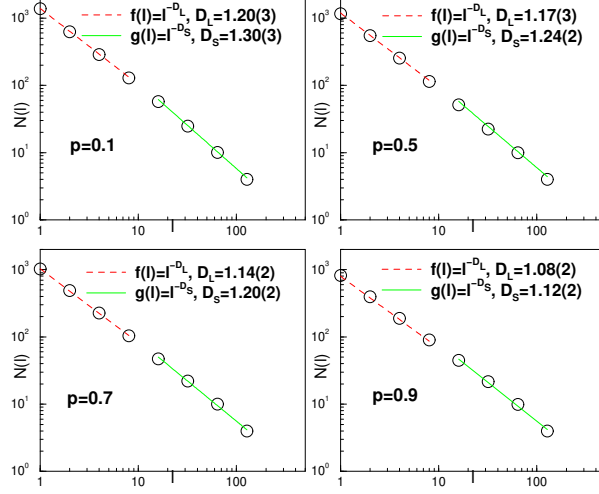


Fig. 3. – (a)-(d): Scaling behavior of the number of occupied boxes  $N(l)$  of size  $l$  versus  $l$ , for different values of  $p$ , horizontal size  $L = 256, 512$  and height  $h = 2L$ . The box counting is made on a strip of height  $h = L/2$ .

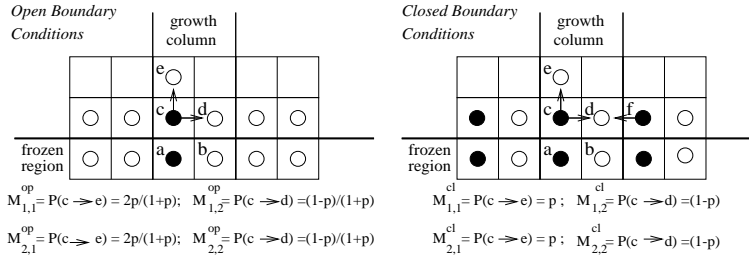


Fig. 4. – Lattice path integrals for the two types of boundary conditions considered. Please note that both in OBC than in the CBC, all the processes starting from configuration of the type  $C_2$  gives the same results of processes starting from configuration  $C_1$ . In fact, if one consider the site  $b$  black, it is impossible to have growth process starting from it, since the Laplacian operator in the point is negative